Development 137, 3119-3128 (2010) doi:10.1242/dev.048785

Moesin1 and Ve-cadherin are required in endothelial cells during in vivo tubulogenesis

Ying Wang[1], Mark S. Kaiser[2], Jon D. Larson[3,4], Aidas Nasevicius[4], Karl J. Clark[4,5], Shannon A. Wadman[4], Sharon E. Roberg-Perez[4], Stephen C. Ekker[5], Perry B. Hackett[3,4], Maura McGrail[1] and Jeffrey J. Essner[1,*]

SUMMARY

Endothelial tubulogenesis is a crucial step in the formation of functional blood vessels during angiogenesis and vasculogenesis. Here, we use in vivo imaging of living zebrafish embryos expressing fluorescent fusion proteins of β-Actin, α-Catenin, and the ERM family member Moesin1 (Moesin a), to define a novel cord hollowing process that occurs during the initial stages of tubulogenesis in intersegmental vessels (ISVs) in the embryo. We show that the primary lumen elongates along cell junctions between at least two endothelial cells during embryonic angiogenesis. Moesin1-EGFP is enriched around structures that resemble intracellular vacuoles, which fuse with the luminal membrane during expansion of the primary lumen. Analysis of *silent heart* mutant embryos shows that initial lumen formation in the ISVs is not dependent on blood flow; however, stabilization of a newly formed lumen is dependent upon blood flow. Zebrafish *moesin1* knockdown and cell transplantation experiments demonstrate that Moesin1 is required in the endothelial cells of the ISVs for in vivo lumen formation. Our analyses suggest that Moesin1 contributes to the maintenance of apical/basal cell polarity of the ISVs as defined by adherens junctions. Knockdown of the adherens junction protein Ve-cadherin disrupts formation of the apical membrane and lumen in a cell-autonomous manner. We suggest that Ve-cadherin and Moesin1 function to establish and maintain apical/basal polarity during multicellular lumen formation in the ISVs.

KEY WORDS: Zebrafish, Endothelial tubulogenesis, Angiogenesis, Lumen, Vacuole, Actin, Moesin1 (Moesin a), Ve-cadherin

INTRODUCTION

The formation of endothelial tubes that transport blood during development is crucial for the normal physiology of large multicellular organisms. Although the pathways involved in the generation of epithelial tubes are well known for kidney and gut (Andrew and Ewald, 2010; Bagnat et al., 2007; Lubarsky and Krasnow, 2003; Martin-Belmonte and Mostov, 2008), less is known about how endothelial cells acquire apical/basal polarity and about the mechanisms that guide formation of the blood vessel lumen (Davis et al., 2007). In addition, recent studies suggest that different blood vessels may form endothelial tubes using distinct mechanisms that include cell hollowing (Ellertsdottir et al., 2009; Kamei et al., 2006), budding (Huisken and Stainier, 2009), sprouting (Herbert et al., 2009) and chord hollowing (Jin et al., 2005). Previous in vitro studies using three-dimensional cultures of human umbilical vein endothelial cells (HUVECs) have shown that intracellular vacuoles generated from pinocytosis fuse to form a primary vessel lumen (Davis and Camarillo, 1996; Folkman and Haudenschild, 1980). Signaling mediated by Cdc42 and Rac1, key G-protein regulators of the Actin cytoskeleton and cell polarity, is crucial for the generation of vacuoles that form the primary lumen and for endothelial tubulogenesis in vitro (Bayless and Davis, 2002; Bayless and Davis, 2004; Koh et al., 2008). Consistent with this requirement, a fusion protein between EGFP and Cdc42 localizes to the membranes of intracellular vacuoles both in vitro and in zebrafish embryos as they fuse and form the primary vessel lumen (Bayless and Davis, 2002; Kamei et al., 2006). These studies have led to a model whereby the lumen of endothelial tubes is formed through the generation of Actin-based polarity and transport of vacuoles to a central cellular position where they fuse to 'hollow out' the luminal surface (Ellertsdottir et al., 2009; Kamei et al., 2006; Lubarsky and Krasnow, 2003).

During tubulogenesis of the zebrafish intersegmental vessels (ISVs), the endothelial cells migrate over one another, divide, and make extensive adherens and tight junctions along the length of the vessel (Blum et al., 2008; Siekmann and Lawson, 2007). Adherens and tight junctions provide cell-to-cell adhesion and serve as a boundary between apical and basolateral membranes in endothelial cells (Dejana et al., 2009a; Dejana et al., 2009b). The importance of adherens junctions during lumen formation is underscored by in vitro studies using HUVECs that show that antibodies against Ve-cadherin (Cadherin 5), the primary adherens junction cadherin in endothelial cells, inhibit lumen formation by preventing vacuole generation and fusion (Yang et al., 1999). The mouse knockout of Ve-cadherin also demonstrates its requirement in the maturation of endothelial cells into functional vascular tubes (Carmeliet et al., 1999; Gory-Faure et al., 1999). Similarly, Ve-cadherin knockdown in zebrafish results in a failure to establish a functional circulatory system (Montero-Balaguer et al., 2009; Nicoli et al., 2007). Therefore, in contrast to the cell hollowing model for tubulogenesis outlined above, the junctions that form between the endothelial cells as they migrate over one another and undergo shape changes could directly define luminal and abluminal membrane domains

[1]Department of Genetics, Development and Cell Biology, Iowa State University, Ames, IA 50011, USA. [2]Department of Statistics, Iowa State University, Ames, IA 50011, USA. [3]Department of Genetics, Cell Biology, and Development, University of Minnesota, Minneapolis, MN 55455, USA. [4]Discovery Genomics Inc., Minneapolis, MN 55413, USA. [5]Department of Biochemistry and Molecular Biology, Mayo Clinic, Rochester, MN 55902, USA.

*Author for correspondence (jessner@iastate.edu)

Accepted 9 July 2010

during tubulogenesis in vivo. Consistent with this idea, a recent report suggests that the luminal membrane in the mouse dorsal aorta is formed by the establishment of junctional contacts between endothelial cells without the contribution of vacuoles to the apical membrane (Strilic et al., 2009).

Members of the Ezrin/Radixin/Moesin (ERM) gene family function in tubulogenesis and apical/basal polarity in diverse organisms (Bretscher et al., 2002; Hughes and Fehon, 2007), probably through their roles in apical membrane biogenesis, adherens junction stabilization and membrane trafficking (Chorna-Ornan et al., 2005; Gobel et al., 2004; Niggli and Rossy, 2008; Saotome et al., 2004; Tamura et al., 2005; Van Furden et al., 2004). ERM proteins have a C-terminal Actin-binding domain and an N-terminal FERM (four-point-one ERM) domain, which is responsible for interaction with apical membrane proteins and phosphatidylinositol 4,5-bisphosphate (PIP2). ERM proteins are present in the cytoplasm in an inactive form and are activated by phosphorylation of a conserved threonine near their C-terminus, resulting in their ability to associate with both Actin and membranes. A number of signaling cascades have been shown to phosphorylate ERM proteins, including the small GTPases Rho and Cdc42, Rho-associated kinase and protein kinase C (Matsui et al., 1998; Nakamura et al., 2000; Ng et al., 2001; Shaw et al., 1998). Consistent with their roles in the organization of the apical membrane, ERM proteins are localized to the Actin-rich apical membrane in epithelial cells, and Moesin is found at the apical surface of endothelial cells (Berryman et al., 1993; Bretscher et al., 2002; Strilic et al., 2009).

In this study, we use transgenic zebrafish expressing Moesin1-EGFP, mCherry-β-Actin and α-Catenin-EGFP fusion proteins to identify a novel multicellular mechanism for endothelial tube formation during embryonic angiogenesis. Using these lines, we can follow formation of the lumen, intracellular vacuoles and sites of cell-cell interaction. Moesin1 (Moesin a – Zebrafish Information Network) and Ve-cadherin are both required for the formation of the vessel lumen and affect the localization of one another. Based on our analysis, we propose that Ve-cadherin-based adherens junctions stabilized by Moesin1 provide apical/basal polarity to the forming vascular tubes in the ISVs.

MATERIALS AND METHODS

Animals

Wild-type strains, wt and WIK, were obtained from 5-D Tropical (Florida) and the Zebrafish International Resource Center (ZIRC), respectively. The *Tg(fli1:egfp)*^{y1} transgenic line was obtained from ZIRC (Lawson and Weinstein, 2002). The *silent heart* mutant used in this study was isolated in a Tol2 transposon insertional mutagenesis screen (Dr Darius Balciunas, Temple University). Homozygous mutant *silent heart* embryos lack a heartbeat, similar to previously identified alleles (Chen et al., 1996). *Tg(flk1:moesin1-egfp)*, *Tg(flk1:mCherry-β-actin)*, *Tg(flk1:α-catenin-egfp)*, *Tg(flk1:nlsmCherry)*, *Tg(flk1:mCherry)* and *Tg(β-actin:rfp)* transgenic lines were generated in our laboratory (http://www.gdcb.iastate.edu/faculty_and_research/bios/jessner.shtml). The GenBank accessions for *moesin1*, *β-actin* and *α-catenin* are NM_001004296, NM_131031 and NM_131456, respectively.

Morpholino (MO) knockdown

moesin1 was identified as being required for vascular development in an MO-based reverse genetic screen in zebrafish. Three MOs (GeneTools) were designed to inhibit the translation of *moesin1*: *moesin1* MO1 5′-TTCGGCATTTTGTCGGTATCTGGTC-3′, *moesin1* MO2 5′-CGGCATTTTGTCGGTATCTGGTCTC-3′ and *moesin1* MO3 5′-ACGAATGTGTCACAAACTGAAGCTG-3′. All three MOs produced similar phenotypes (data not shown). The *moesin1* MO1 was used for all experiments shown. A splice-site-directed MO was designed to inhibit the pre-mRNA splicing between exons 10 and 11 of *ve-cadherin* (GenBank accession NM_001003983): *ve-cadherin* MO 5′-AGATGAACCT-ACCCAGGATGGTAAT-3′. Unless otherwise noted, 4 ng of *moesin1* MO, 10 ng of *ve-cadherin* MO, or 10 ng of random sequence control MO was injected into one-cell stage embryos.

Transplantation

Approximately 20 marginal cells were transplanted at dome stage. Both the donor and recipient embryos were *Tg(fli1:egfp)*^{y1} transgenic carriers, allowing visualization of all endothelial cells by detection of EGFP fluorescence. Additionally, the donor embryos were progeny from a cross between *Tg(β-actin:rfp)* and *Tg(fli1:egfp)*^{y1}, which allowed us to follow all transplanted cells and distinguish the transplanted ISVs from non-transplanted ISVs by detection of RFP fluorescence. With this technique, ~10% of the recipient embryos displayed ISVs from transplanted cells. Each recipient embryo with transplanted cells was scored for morphology (lumen formation) and blood circulation (blood cells going through) in the EGFP/RFP double-fluorescent ISVs at 54 hours post-fertilization (hpf) using a Carl Zeiss SteREO Discovery V.12 microscope. Donor embryos (n=20) were kept and scored at 54 hpf to confirm that the expected defects in tubulogenesis were detected after MO injection.

Immunofluorescence

The anti-ZO-1 monoclonal antibody (Zymed) was used at 1:200 dilution. The zebrafish anti-Ve-cadherin antibody (Blum et al., 2008) was used at 1:500. Alexa 594-labeled goat anti-mouse and Alexa 594-labeled goat anti-rabbit secondary antibodies (Molecular Probes) were used at 1:1000.

Microangiography

Microangiography was carried out as described (Kalen et al., 2009).

Confocal imaging

Living zebrafish embryos were mounted in 1% low-melting agarose on a coverslip and imaged with a 20× objective (0.7 NA) on a Leica TCS SP5 X confocal microscope or with a 25× objective (0.75 NA) on a Leica TCS NT confocal microscope. Images of fixed embryos were obtained with a 63× oil-immersion objective (1.32 NA) using a Leica TCS NT confocal microscope. Fixed zebrafish embryos were mounted in aqueous mounting medium with anti-fading agents (Biomeda). Images were analyzed with MetaMorph 6.1 (Universal Imaging) or Imaris 7.0 (Bitplane) software. All images represent a compressed z-series.

RESULTS

Formation of the vessel lumen during embryonic angiogenesis

We generated transgenic zebrafish lines to follow lumen formation in the vascular system. These lines, which express Moesin1-EGFP and mCherry-β-Actin fusion proteins specifically in endothelial cells using the *flk1* (*kdrl* – Zebrafish Information Network) promoter (Jin et al., 2005), are named *Tg(flk1:moesin1-egfp)* and *Tg(flk1:mCherry-β-actin)*, respectively. In polarized epithelial and endothelial cells, Moesin and Actin are enriched at both the apical membrane and adherens junctions (Bretscher et al., 2002; Strilic et al., 2009). Similar patterns of localization for Moesin1-EGFP and mCherry-β-Actin fusion proteins were observed in epithelial cells in the zebrafish otic vesicle (see Fig. S1 in the supplementary material). Additionally, mCherry-β-Actin localized to putative Actin filaments in the periderm (see Fig. S1 in the supplementary material).

We next examined the ISVs in the transgenic lines to see whether the fusion proteins would allow us to follow changes in polarity during the process of tubulogenesis. The capillary-like ISVs form during the first wave of embryonic angiogenesis by migration of endothelial cells dorsally from the aorta (Isogai et al., 2001; Isogai et al., 2003; Kamei et al., 2006) (Fig. 1A). During

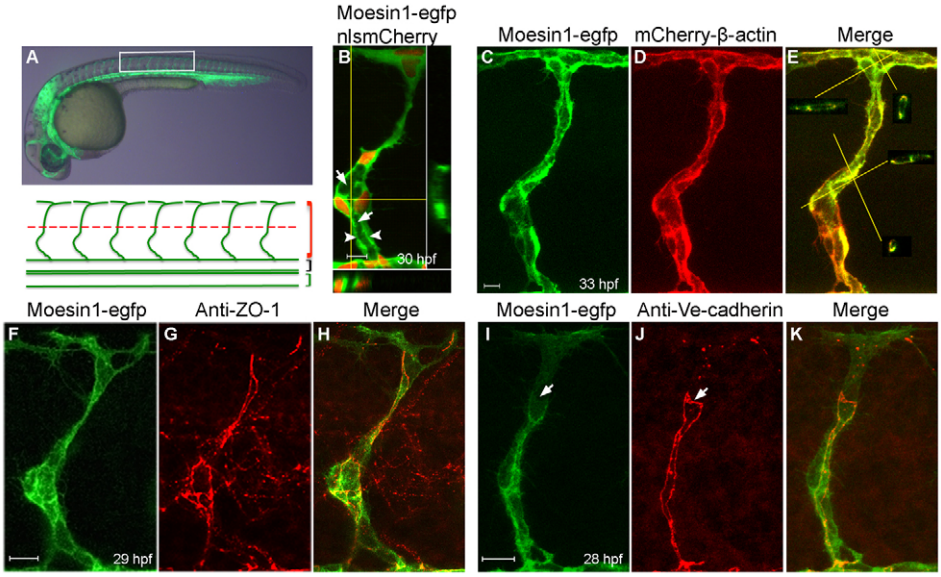

Fig. 1. Moesin1-EGFP and mCherry-β-Actin fusion proteins are enriched at apical membranes and cellular junctions. (**A**) A 30 hpf zebrafish embryo from *Tg(flk1:moesin1-egfp)* with the box indicating the area shown beneath. Red, black and green brackets indicate the intersegmental vessels (ISVs), dorsal aorta (DA) and posterior caudal vein (PCV), respectively. The red dashed line designates the boundary between the dorsal (top) or ventral (bottom) ISVs. (**B**) An ISV in a *Tg(flk1:moesin1-egfp)/Tg(flk1:nlsmCherry)* embryo showing the primary lumen (arrows) forming at 30 hpf. Moesin1-EGFP is enriched at the apical membrane (arrowheads). The nuclei are in red. Virtual cross-sections are at the bottom and to the right of the main panel. Yellow lines designate the planes of the cross-sections. (**C-E**) A *Tg(flk1:moesin1-egfp)/Tg(flk1:mCherry-β-actin)* embryo at 33 hpf displayed considerable overlap of fluorescence in the ISV. Virtual cross-sections in E show the lumen. (**F-H**) Moesin1-EGFP and the tight junction protein ZO-1 co-localized at 29 hpf. (**I-K**) At 28 hpf, Moesin1-EGFP is enriched at adherens junctions, as labeled with anti-Ve-cadherin antibody, although not always (arrows). (A-K) Lateral images, dorsal is up, anterior is to the left. Scale bars: 10 μm in all figures.

early endothelial tube formation of the ISVs (28 to 33 hpf), the Moesin1-EGFP fusion protein became enriched at the apical membrane as the primary lumen formed, thus highlighting the forming lumen (Fig. 1B-E; see Movies 1 and 2 in the supplementary material). Here, we define the primary lumen as the initial lumen that forms in the ISVs prior to the initiation of circulation. By comparison, embryos from the *Tg(fli1:egfp)*^{y1} line (Lawson and Weinstein, 2002) that express EGFP in the endothelial cells did not show specific subcellular localization and did not illustrate the initial stages of tubulogenesis (see Fig. S2 in the supplementary material). Furthermore, the *Tg(flk1:nlsmCherry)* line that targets a red fluorescent protein (RFP) to the nucleus demonstrated that the primary lumen highlighted by the Moesin1-EGFP protein was distinct from nuclei (Fig. 1B). Consistent with the role of Moesin1 as an Actin-binding protein, Moesin1-EGFP and mCherry-β-Actin appeared to show a similar pattern of localization (Fig. 1C-E).

Similar to previous reports (Blum et al., 2008), ZO-1 (Tjp1 – Zebrafish Information Network) and Ve-cadherin localized to long junctions that run lengthwise along the ISVs at 30 hpf (Fig. 1F-K). As the endothelial cells migrate over one another during primary lumen formation in the ISVs, at least two junctional sites were observed between the cells, indicating that there were two connected cells. Fixation of the embryos is likely to remove much of the cytoplasmic signal from the *Tg(flk1:moesin1-egfp)* line, as much of the cytoplasmic Moesin protein is in an inactive and soluble state. In fixed embryos, the fluorescence from Moesin1-EGFP was enriched at sites defined by the localization of the tight junction protein ZO-1 and the vascular-specific adherens junction protein Ve-cadherin (Fig. 1F-K). However, Moesin1-EGFP was not detected at all positions where Ve-cadherin labeling was present (Fig. 1I-K).

Our results suggest that the luminal membrane acquires polarity and the primary lumen forms in regions defined by cellular junctions between at least two endothelial cells, as opposed to a single-cell hollowing mechanism. To address this idea and follow the adherens junctions in living embryos, we generated a *Tg(flk1:α-catenin-egfp)* transgenic line that expresses α-Catenin-EGFP in the endothelial cells. α-Catenin is a cytoplasmic cadherin-binding protein that localizes to adherens junctions. In addition to cytoplasmic detection of EGFP throughout the ISV, we observed localization of α-Catenin-EGFP to putative junctional sites within ISVs (Fig. 2A-C). We confirmed the localization of α-Catenin-EGFP to adherens junctions by probing with Ve-cadherin antibodies (Fig. 2D-F). In addition, α-Catenin-EGFP showed nuclear localization similar to that in the *Tg(flk1:nlsmCherry)* line (Fig. 2D-F). To follow adherens junctions and primary lumen formation at the same time, we crossed *Tg(flk1:α-catenin-egfp)* with a *Tg(flk1:mCherry)* line. Using time-lapse confocal microscopy, we observed that α-Catenin-EGFP was associated with the putative primary lumen in the ventral region of the ISV (Fig. 2G, arrows). In the dorsal part of the ISV, α-Catenin-EGFP-positive structures expanded from ventral to dorsal, possibly defining the forming lumen (Fig. 2G and see Movie 3 in the supplementary material). Taken together, our analyses suggest that cellular junctions form between cells and define the primary lumen in the ISVs.

Intracellular vacuoles fuse with luminal membranes during formation of the primary lumen

Similar to EGFP-Cdc42 fusion proteins (Kamei et al., 2006), the Moesin1-EGFP fusion protein is also observed surrounding vesicle-like structures, termed vacuoles, during endothelial tubulogenesis. To

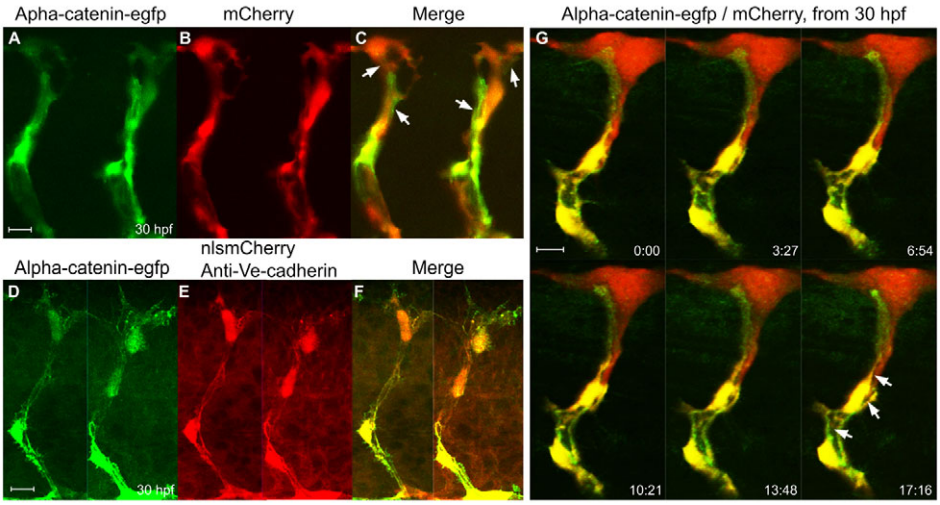

Fig. 2. α-Catenin-EGFP localizes to adherens junctions associated with the primary lumen in the ISVs. (**A-C**) Confocal images of the ISVs in a living *Tg(flk1:α-catenin-egfp)/Tg(flk1:mCherry)* zebrafish embryo at 30 hpf. Arrows in C point to long putative adherens junctions between cells. (**D-F**) Labeling of adherens junctions in the ISVs with anti-Ve-cadherin antibody in a *Tg(flk1:α-catenin-egfp)/Tg(flk1:nlsmCherry)* double-transgenic embryo. (**G**) Time-lapse confocal images of an ISV in a *Tg(flk1:α-catenin-egfp)/Tg(flk1:mCherry)* embryo showing the putative primary lumen (arrows) forming between the cellular junctions. The time format is minutes:seconds.

determine whether these vacuoles contribute to lumen formation, we performed time-lapse confocal microscopy with the *Tg(flk1:moesin1-egfp)/Tg(flk1:nlsmCherry)* double-transgenic embryos. At 30 hpf, the endothelial cells of the ISVs completed their dorsal migration and initiate tube formation in the ventral half of the ISV. In the dorsal half of the ISV, lumens were observed to form and expand within seconds to minutes (see Movies 1 and 2 in the supplementary material). Vacuoles (1.08 μm in diameter; s.d.=0.29, *n*=21) were observed fusing with the luminal membrane (Fig. 3A,B and see Movie 2 in the supplementary material). The vacuoles were extremely dynamic and fused to the lumen within seconds of their appearance. The active trafficking of vacuoles was also present in the ventral ISVs at a slightly earlier stage, at 28 hpf (see Movie 4 in the supplementary material).

To ensure that the Moesin1-EGFP-labeled vacuoles are not simply invaginations of the primary luminal membrane, high-molecular-weight tetramethylrhodamine-dextran (TMRD) was injected intravenously into the sinus venosus of 30 hpf embryos to highlight the forming lumen. Vacuoles that did not contain TMRD were present near the forming primary lumen (Fig. 3C,D and see Movie 5 in the supplementary material), suggesting that these vacuoles do not originate from the luminal membrane. However, TMDR was observed in other invaginations. These could be interpreted as vacuoles that have recently fused to the lumen, or as the movement of luminal membranes during lumen expansion. The extent to which the luminal membrane is derived from the vacuoles is currently unknown, but sites of lumen expansion correlate with the presence of vacuoles.

In contrast to the ISVs, vacuoles were not observed in the endothelial cells in the dorsal aorta at 18 hpf, when it is undergoing tubulogenesis (see Movie 6 in the supplementary material), consistent with previous studies in mice (Strilic et al., 2009). Our analyses show cells of the dorsal aorta moving relative to one another and elongating (see Movie 6 in the supplementary material). These results suggest that different vascular beds utilize distinct mechanisms for creating the lumen during tubulogenesis and large vacuoles are not utilized in all mechanisms.

Blood flow is not required for primary lumen formation

Numerous studies have shown that blood flow is required for the maintenance of functional vessels; however, the contribution of blood flow to endothelial tubulogenesis is not well understood. From the TMRD injections above, we observed that the ventral half of the ISV undergoes initial lumen formation in the absence of perfusion (data not shown), suggesting that initial tube formation is not dependent on blood flow. To test this, we crossed the *Tg(flk1:moesin1-egfp)* line to an allele of *silent heart*. *silent heart* mutants have a mutation in *cardiac troponin T2a* and consequently fail to establish a heartbeat and blood circulation (Chen et al., 1996; Sehnert et al., 2002). Previous reports have shown that the endothelial cells in the ISVs migrate normally in *silent heart* mutant embryos in the absence of blood flow (Isogai et al., 2003).

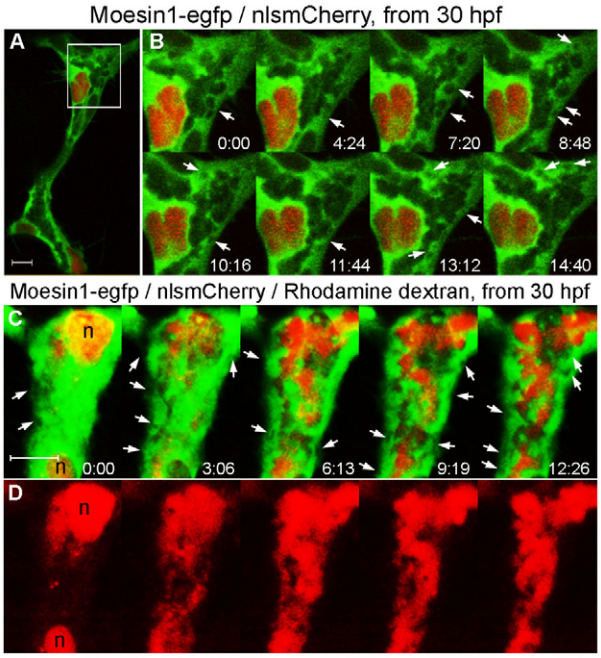

Fig. 3. Vacuoles fuse with luminal membranes during initial lumen expansion. (**A**) An ISV from a living *Tg(flk1:moesin1-egfp)/Tg(flk1:nlsmCherry)* zebrafish embryo with the box indicating the area shown in B. (**B**) Time-lapse confocal images showing formation of primary lumen in an ISV with the integration of vacuoles (arrows) from 30 hpf. (**C**,**D**) A dorsal ISV from a living *Tg(flk1:moesin1-egfp)/Tg(flk1:nlsmCherry)* embryo injected intravenously with labeled dextran (D) showing the intracellular vacuoles without labeled dextran (C, arrows). The time is in minutes:seconds. n, nucleus.

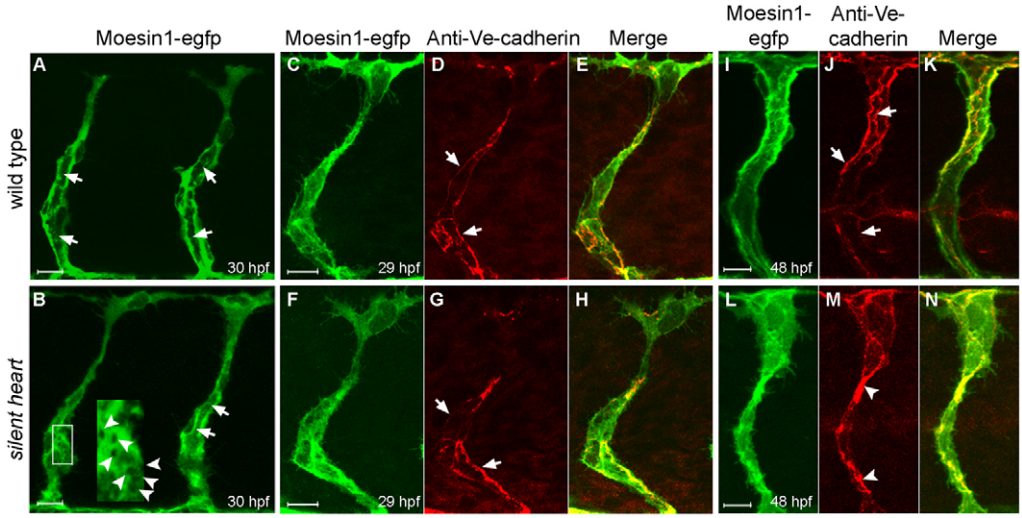

Fig. 4. Primary endothelial lumen formation in the ISVs does not require blood flow. (**A**,**B**) Formation of the primary lumen (arrows) at 30 hpf is observed with the *Tg(flk1:moesin1-egfp)* line in either wild-type (A) or *silent heart* mutants (B). (B) *silent heart* embryos also displayed vacuoles during tubulogenesis (arrowheads in inset). (**C-H**) Ve-cadherin-labeled junctions (arrows) appeared normal at 29 hpf in *silent heart* mutants. (**I-N**) At 48 hpf, Ve-cadherin-labeled junctions (arrows) are often clustered in the *silent heart* embryos (arrowheads), which is likely to reflect the collapse of the primary lumen.

The endothelial cells in the ISVs initiated tubulogenesis by 30 hpf in the *silent heart* mutant embryos, with both primary lumen formation (58% of ISVs, n=19 ISVs) and the presence of vacuoles (75% of ISVs, n=4) detected within the ventral ISVs (Fig. 4A,B). The Ve-cadherin-based adherens junctions were normal during these initial stages of tubulogenesis (100% of ISVs, n=7) (Fig. 4C-H). At 48 hpf, when wild-type embryos have formed a functional lumen in the ISVs, the initial lumens that were observed at 30 hpf in the *silent heart* embryos collapsed (69% of ISVs, n=9) (Fig. 4I-N). Consistent with this, Ve-cadherin labeling of the *silent heart* embryos at 48 hpf showed that the adherens junctions were very close to one another in the ventral region of the ISVs. Similar to previous reports (Isogai et al., 2003), the endothelial cells in the dorsal regions of the ISVs became enlarged. However, TUNEL labeling at this time did not reveal increased apoptosis of the endothelial cells (data not shown). Together, these observations indicate that initial endothelial tubulogenesis in the ISVs is independent of blood flow, but maintenance of the lumen in the vessel is dependent upon blood flow.

Moesin1 is required in the endothelial cells for ISV tubulogenesis

Zebrafish *moesin1* is expressed in the endothelial cells throughout the vasculature, as well as in the anterior central nervous system and the somite (data not shown). *moesin1* was knocked down in embryos using a morpholino (MO) directed at the first AUG. Microangiography performed at 39, 54 and 78 hpf showed that most ISVs in the knockdown embryos did not transfer labeled dextran from the dorsal aorta (see Fig. S3 in the supplementary material), indicating there is a tube formation defect that is not merely a result of developmental delay. The defect observed after knockdown of Moesin1 displayed strong dose dependence in both the axial vessels and the ISVs (see Fig. S4 in the supplementary material). Similar to observations in mice (Strilic et al., 2009), tubulogenesis of the dorsal aorta and caudal vein was weakly affected following knockdown of Moesin1. Furthermore, knockdown of Moesin1 did not significantly affect endothelial cell migration in the ISVs (see Fig. S3 in the supplementary material) or cell number at 30 hpf (data not shown). Taken together, these data support a role for *moesin1* in endothelial tubulogenesis during embryonic angiogenesis.

Moesin1 knockdown embryos also displayed an overall smaller size, edema in the pericardial and yolk compartments, and cell death in the anterior central nervous system (see Fig. S3 in the supplementary material). Western blot analysis confirmed that *moesin1* MO strongly reduced Moesin1 protein levels during early zebrafish development (see Fig. S4 in the supplementary material). The Moesin1 knockdown phenotypes were observed after injection of three different AUG-directed MOs, suggesting specificity of the MOs for the *moesin1* mRNA. The circulation defects caused by loss of Moesin1 were not rescued by p53 knockdown, excluding the possibility that the vascular tube formation defects in Moesin1 knockdown embryos are a side effect of induction of the *p53*-dependent cell death pathway (data not shown).

The *Tg(flk1:moesin1-egfp)* transgene was engineered with the *flk1* 5′UTR so that MOs directed against endogenous Moesin1 would not recognize the *moesin1-egfp* transgene mRNA. This allowed us to test whether Moesin1-EGFP can rescue the Moesin1 knockdown phenotype specifically in the endothelial cells. A control or *moesin1* MO was injected into embryos from a heterozygotic *Tg(flk1:moesin1-egfp)* zebrafish outcrossed with wild type and microangiography was performed at 54 hpf (Fig. 5A-F and see Fig. S5 in the supplementary material). Whereas the non-transgenic embryos displayed strong ISV tube defects after injection of the *moesin1* MO (Fig. 5C,D), these defects were reduced in transgenic *Tg(flk1:moesin1-egfp)* siblings (P<0.01) (Fig. 5E,F; see Table S1 in the supplementary material). In addition, the same experiment was performed for embryos from a heterozygotic *Tg(flk1:moesin1-egfp)* zebrafish crossed with *Tg(flk1:nlsmCherry)*, and demonstrated the presence of ISV endothelial cells in both *Tg(flk1:moesin1-egfp)*/*Tg(flk1:nlsmCherry)* double-transgenic embryos and *Tg(flk1:nlsmCherry)* embryos following the injection of *moesin1* MO (Fig. 5G-I). These data demonstrate that Moesin1-EGFP is a functional protein and that Moesin1 is required within the endothelial cells for ISV tube formation.

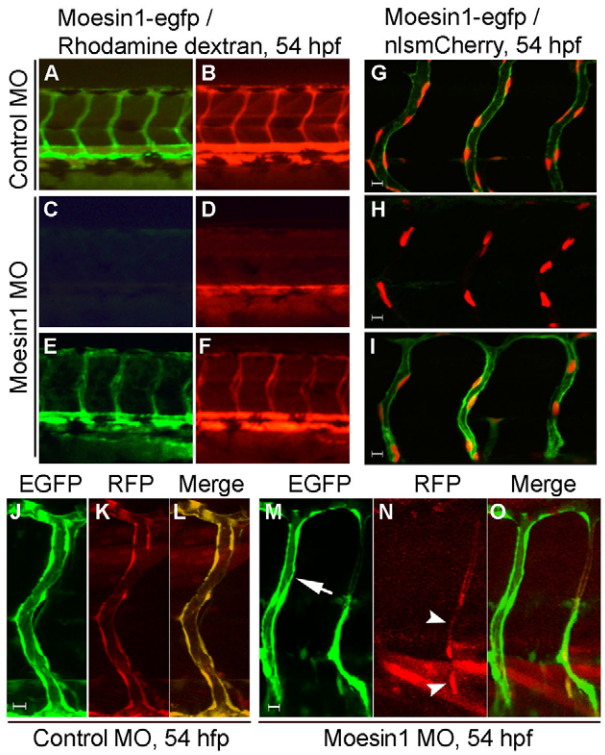

Fig. 5. Moesin1 is required in the endothelial cells for tubulogenesis. (**A-F**) The *Tg(flk1:moesin1-egfp)* line partially rescues the Moesin1 knockdown phenotype. (A,B) A *Tg(flk1:moesin1-egfp)* zebrafish embryo injected with 4 ng control MO. All the ISVs were perfused with tetramethylrhodamine-dextran (TMRD, red). (C,D) Wild-type sibling embryo injected with 4 ng *moesin1* MO. Most ISVs are not perfused with TMRD, although circulation of TMRD is observed in the axial vessels. (E,F) A *Tg(flk1:moesin1-egfp)* embryo injected with 4 ng *moesin1* MO. Most ISVs are perfused with TMRD. (**G-I**) Same experiment as in A-F in *Tg(flk1:moesin1-egfp)/Tg(flk1:nlsmCherry)* embryos shows that the endothelial cells are present in the ISVs despite a lack of circulation at 54 hpf. (**J-O**) Transplantation of endothelial cells was used to determine autonomous verses non-autonomous effects. (J-L) Normal endothelial tubulogenesis occurs when the donor embryo was injected with control MO. (M-O) Transplanted endothelial cells from Moesin1 knockdown embryos fail to undergo normal tubulogenesis (arrowheads), whereas the ISV in the recipient embryo (arrow) completes lumen formation.

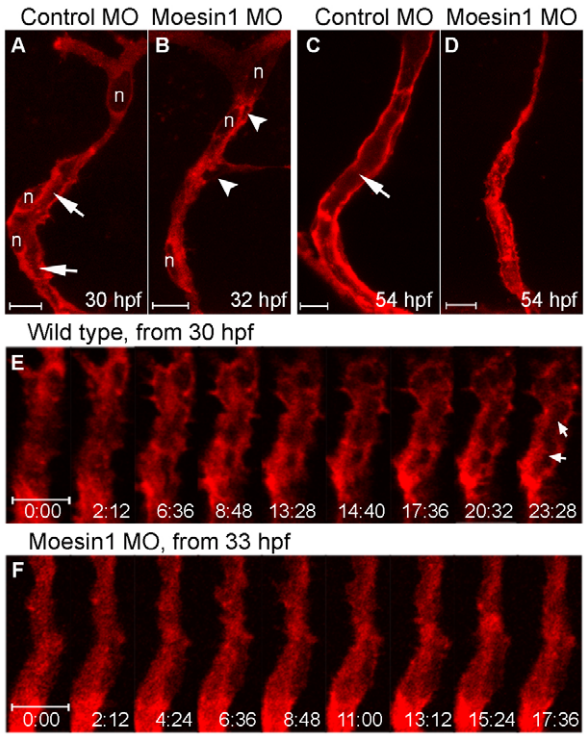

Fig. 6. Moesin1 is required during ISVs tubulogenesis. (**A-D**) Confocal images of ISVs from *Tg(flk1:mCherry-β-actin)* living zebrafish embryos. (A,C) Embryos injected with 4 ng control MO. The lumen (arrows) is seen at 30 hpf (A) and is well formed at 54 hpf (C). (B,D) Embryos injected with 4 ng *moesin1* MO. The primary lumen is not observed at 32 hpf (B), nor at 54 hpf (D), although a few putative vacuoles or intercellular spaces are observed (B, arrowheads). (**E**,**F**) Confocal time-lapse images of wild-type and Moesin1 knockdown *Tg(flk1:mCherry-β-actin)* embryos. The time format is minutes:seconds. (E) In wild-type embryos, formation of the primary lumen is observed (arrows) at 30 hpf. (F) In Moesin1 knockdown embryos, mCherry-β-Actin remains throughout the cytoplasm and the primary lumen is not observed at 33 hpf. n, nucleus.

To test whether the Moesin1 tube formation phenotype is cell autonomous, cell transplantation was performed to follow the effects of Moesin1 knockdown in individual, and groups of, ISV cells. Transplanted endothelial cells from control MO-injected embryos formed normal ISVs (Fig. 5J-L). By contrast, the transplanted Moesin1 knockdown ISVs were narrow and failed to form an expanded lumen at 54 hpf ($P<0.02$) (Fig. 5M-O; see Table S2 in the supplementary material). This result indicates that Moesin1 functions in a cell-autonomous manner in the ISVs during tubulogenesis and that the defects in Moesin1 knockdown embryos are not caused by a secondary effect, such as reduced blood flow in the dorsal aorta.

Knockdown of Moesin1 impairs formation of the luminal membrane

We next examined the effects of Moesin1 knockdown during tubulogenesis using *Tg(flk1:mCherry-β-actin)* embryos to follow the formation of the luminal membrane. In control MO-injected embryos, primary lumen formation was well underway at 30 hpf (75% of ISVs, $n=4$ ISVs) (Fig. 6A,E and see Movie 7 in the supplementary material), and functional ISVs with well-defined lumens were observed in *Tg(flk1:mCherry-β-actin)* transgenics at 54 hpf (100% of ISVs, $n=3$) (Fig. 6C). By contrast, no primary lumen was observed at 32-33 hpf for Moesin1 knockdown embryos when the endothelial cells had migrated to their dorsal extent as in control embryos (86% of ISVs, $n=7$) (Fig. 6B,F and see Movie 8 in the supplementary material). At 54 hpf, the ISVs lacked a visible lumen in Moesin1 knockdown embryos, with the ISVs having a narrow appearance and disorganized mCherry-β-Actin fluorescence through the center of the ISVs (86% of ISVs, $n=7$) (Fig. 6D). These results demonstrate a requirement for Moesin1 in the formation and/or expansion of the luminal membrane during endothelial tubulogenesis.

Moesin1 is required for adherens junctions but not ZO-1-associated junctions

We next investigated whether Moesin1 was required for endothelial cell polarity as defined by tight and adherens junctions. Antibodies against ZO-1 labeled the tight junctions and possibly a subset of adherens junctions in *Tg(fli1:egfp)*^{y1} embryos. A pair of relatively parallel, well-separated ZO-1-associated junctions that run the length

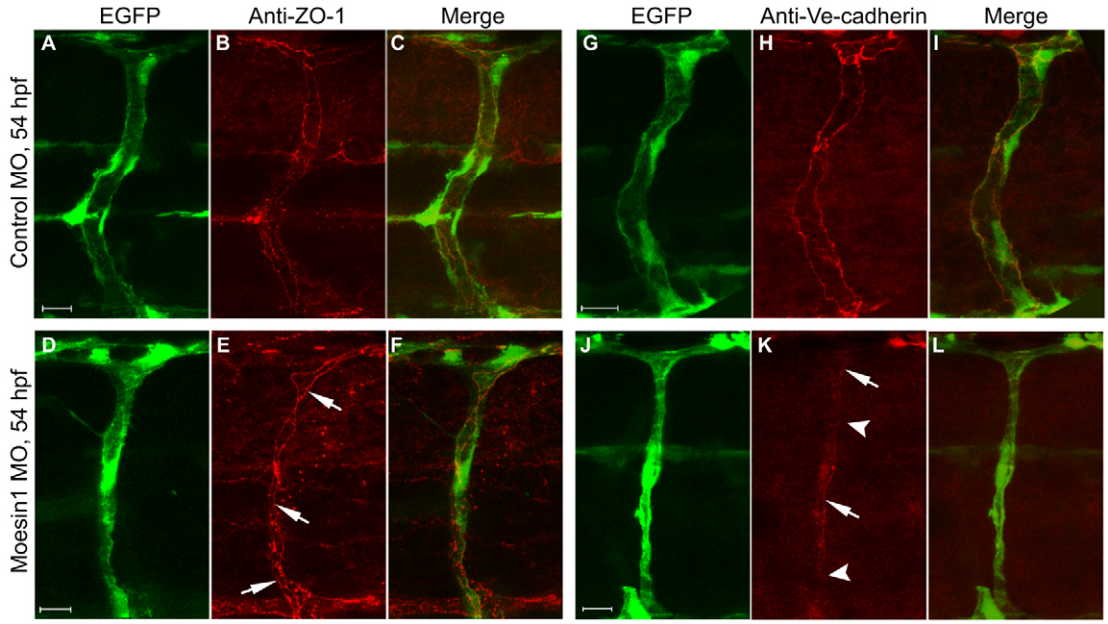

Fig. 7. Knockdown of Moesin1 results in extensive loss of adherens junctions without affecting ZO-1-associated junctions. (**A-F**) Confocal images of ISVs in the *Tg(fli1:egfp)*^{y1} zebrafish embryos that were probed for ZO-1 (red) at 54 hpf. (A-C) ZO-1-associated junctions are seen in a control embryo. (D-F) The ZO-1-associated junctions (arrow) are observed in Moesin1 knockdown embryos but are not well separated from one another. (**G-L**) Confocal images of ISVs in *Tg(fli1:egfp)*^{y1} embryos labeled with Ve-cadherin (red) at 54 hpf. (G-I) Ve-cadherin labeling in a control embryo. (J-L) Moesin1 knockdown causes an extensive loss of Ve-cadherin labeling (arrowheads); some weak Ve-cadherin signals are observed (arrows).

of ISVs was observed in control MO-injected embryos at 34 hpf (83% of ISVs, *n*=6 ISVs) (see Fig. S6A-C in the supplementary material) and 54 hpf (67% of ISVs, *n*=3) (Fig. 7A-C). By contrast, Moesin1 knockdown embryos showed one or two closely opposed ZO-1-associated junctions along the ISVs at 36 hpf (83% of ISVs, *n*=6) (see Fig. S6D-F in the supplementary material) and 54 hpf (67% of ISVs, *n*=3) (Fig. 7D-F). The appearance of a single ZO-1-positive junction might reflect defects in primary lumen formation rather than in the formation of the junction itself, as a failure to expand the lumen would prevent the junctions from becoming separated. Furthermore, the presence of ZO-1-positive junctions suggests that there are still at least two cells along much of the length of ISVs. Thus, the defect in lumen formation is unlikely to be the result of defects in cell number or in migration of the endothelial cells over one another, or due to the lack of ZO-1-positive junction formation.

We examined the effect of Moesin1 knockdown on Ve-cadherin-based adherens junctions by probing with antibodies against Ve-cadherin. In contrast to the results with ZO-1, there was an extensive loss of Ve-cadherin labeling in the ISVs of Moesin1 knockdown embryos. This lack of localization of Ve-cadherin labeling to the putative adherens junctions in the Moesin1 knockdown embryos was apparent at 32 hpf (67% of ISVs, *n*=6 ISVs) (see Fig. S6G-L in the supplementary material) and at 54 hpf (86% of ISVs, *n*=7) (Fig. 7J-L). These results indicate that Moesin1 is required for adherens junction formation and/or stabilization during lumen formation and could also reflect a defect in endothelial apical/basal polarity.

Knockdown of Ve-cadherin impairs ISV lumen formation

We next investigated whether interfering with formation of the Ve-cadherin-based adherens junctions directly would impair ISV tubulogenesis. In Ve-cadherin knockdown embryos, the ISVs appeared to be narrow and lacked visible lumens at 54 hpf (Fig. 8A-F). The efficacy of the *ve-cadherin* MO was verified by RT-PCR (see Fig. S7 in the supplementary material) and immunolabeling with anti-Ve-cadherin antibodies (Fig. 8A-F). The *ve-cadherin* MO-injected embryos displayed a lack of circulation in the axial vessels and ISVs at 56 hpf and did not display an increase in endothelial cells entering into apoptosis when assessed by TUNEL labeling, as compared with control embryos at 30 hpf (data not shown).

We analyzed tight junctions in Ve-cadherin knockdown embryos using the anti-ZO-1 antibody. Most ISVs in the Ve-cadherin knockdown embryos showed some organized ZO-1 labeling. However, the labeling was discontinuous and sometimes did not extend the length of the ISVs. This suggests that at some positions along the ISVs, only one cell is present. Alternatively, more than one cell is present and tight junctions form between the cells, but the junctions fail to extend lengthwise along the entire ISV (Fig. 8G-L). This result indicates that without Ve-cadherin-based junctions, limited tight junctions could still form between endothelial cells that contribute to ISVs. The abnormal ZO-1 labeling patterns suggest that Ve-cadherin is required either for the migration of endothelial cells over one another or for the remodeling of ZO-1-positive junctions into fully extended junctions that define the lumen during tubulogenesis.

We tested whether the absence of circulation in Ve-cadherin knockdown embryos was responsible for producing the defects in ISV tube formation using transplantation experiments as described above for the Moesin1 knockdowns. Individual transplanted endothelial cells from Ve-cadherin knockdown embryos failed to undergo tubulogenesis when transplanted into embryos with normal circulation (P<0.01) (see Fig. S8 and Table S1 in the supplementary material). These results indicate that the defect in

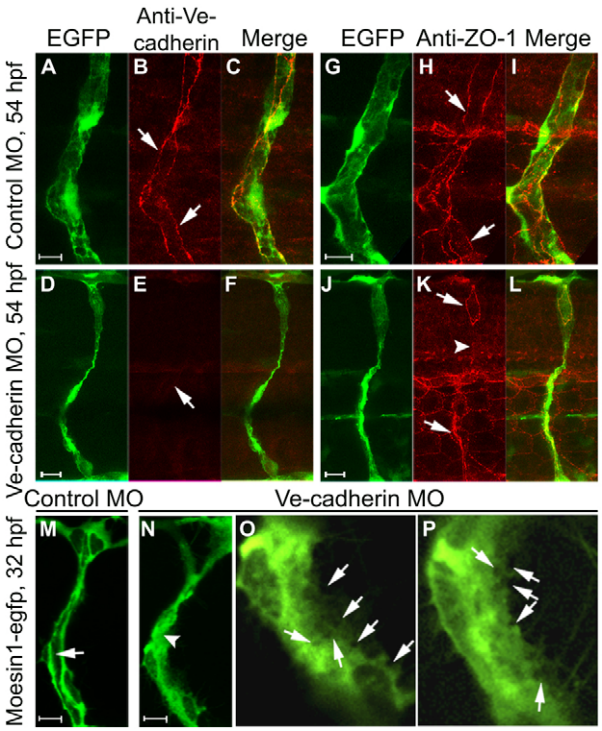

Fig. 8. Knockdown of Ve-cadherin impairs lumen formation. (**A-F**) Confocal images of ISVs in *Tg(fli1:egfp)*^{y1} zebrafish embryos probed for Ve-cadherin (red) at 54 hpf. Ve-cadherin labeling (arrows) is observed in control embryos (A-C), but not in Ve-cadherin knockdown embryos (D-F). (**G-L**) Confocal images of ISVs in *Tg(fli1:egfp)*^{y1} embryos labeled with ZO-1 antibody (red) at 54 hpf. ZO-1-associated junctions (arrows) are observed in control embryos (G-I), but are not detected in some regions of the ISV (arrowhead) in a Ve-cadherin knockdown embryo (J-L). (**M-P**) Confocal images of ISVs in *Tg(flk1:moesin1-egfp)* embryos at 32 hpf. The primary lumen (arrow) is forming in a control embryo (M). Putative vacuoles or intercellular spaces (arrows in the higher magnification images O and P) are observed throughout the cytoplasm in endothelial cells in Ve-cadherin knockdown embryos (N-P), without formation of primary lumen (N, arrowhead).

lumen formation after Ve-cadherin knockdown is not due to a lack of circulation and demonstrate that Ve-cadherin functions in a cell-autonomous manner in the ISVs during tubulogenesis.

To investigate whether Ve-cadherin is required for the localization of Moesin1-EGFP, we examined the effects of Ve-cadherin knockdown in *Tg(flk1:moesin1-egfp)* embryos. Following knockdown of Ve-cadherin, the primary luminal space was absent (Fig. 8M-P). Moesin1-EGFP was not enriched at any sites along the length of the ISVs, indicating that it fails to become polarized in the absence of Ve-cadherin. By 54 hpf, the endothelial cells in Ve-cadherin knockdown embryos in the ISVs appeared to be narrow, similar to those in Moesin1 knockdown embryos. These data suggest that in the absence of Ve-cadherin, the primary lumen fails to form between cells.

DISCUSSION

ISV tube formation occurs by a cord hollowing mechanism

Our results suggest that a cord hollowing mechanism between two endothelial cells is used for ISV tubulogenesis. Our data suggest that two endothelial cells in close contact form adherens junctions that define the future site of the apical membrane. Subsequent apical membrane expansion and lumen formation are likely to be driven in part by the contribution of vacuoles to the apical domain. As the primary lumen is formed, the junctional contacts that define the lumen are elongated lengthwise along the vessel as the endothelial cells migrate over one another. This model is supported by our observation that α-Catenin-EGFP localization defines regions of lumen formation (Fig. 2). In the absence of Ve-cadherin-based adherens junctions, the endothelial cells of the ISVs presumably fail to form the luminal membrane (Fig. 8). The Ve-cadherin-based adherens junctions are likely to designate where the apical membrane should form by creating a physical marker that initially defines apical/basal polarity in the cell.

Ve-cadherin-based adherens junctions are required for ISV tubulogenesis

During embryonic angiogenesis in zebrafish, we show that Ve-cadherin is required for localization of Moesin1-EGFP to the future apical membrane and for lumen formation in the ISVs. The absence of localization of Moesin1-EGFP in Ve-cadherin knockdown embryos might reflect altered cell polarity. ZO-1 localization in Ve-cadherin-deficient endothelial cells indicates that the tight junctions do not extend along the entire length of the ISV, revealing an underlying defect in either the polarity of the endothelial cells or cell migration. These results suggest that as the endothelial cells migrate over one another, the formation of cellular junctions and establishment of cell polarity are tightly coupled to the tubulogenesis process. This could also represent a signaling function for Ve-cadherin. The requirement for Ve-cadherin during endothelial tubulogenesis, both in vitro and in vivo, has long been appreciated (Carmeliet et al., 1999; Gory-Faure et al., 1999; Yang et al., 1999). However, knockout models in mice suggest that endothelial tube defects occur from an inability of cells to adhere to one another. Recent work suggests that Ve-cadherin is required for establishing endothelial polarity during vasculogenesis of the dorsal aorta in mice (Strilic et al., 2009). In this study, in the absence of Ve-cadherin, Moesin and F-actin fail to localize to regions of endothelial cell-cell contact (Strilic et al., 2009). Our work is consistent with these findings and suggests that one function of Moesin1 is downstream of Ve-cadherin during endothelial polarization of the ISVs.

Moesin1 has additional roles during tubulogenesis of the ISVs relating to junction formation and stabilization. We observe two forms of Ve-cadherin-based cellular junctions in endothelial cells (Fig. 1): junctions that are associated with Moesin1-EGFP and are located in more mature regions (the ventral part) of the ISV that have formed a primary lumen; and junctions (the dorsal part) that are not associated with Moesin1-EGFP. The latter might represent newly formed junctions or sites of junctional remodeling as contacts change between the migrating cells. Our analyses show that Moesin1 plays a central role in establishing and/or maintaining the Ve-cadherin-based junctions. A similar relationship between Moesin and E-cadherin has been found in *Drosophila*, in which Moesin is required for the stabilization of E-cadherin junctions in the embryonic epithelium through its interaction with Bitesize, a synaptotagmin-like protein (Pilot et al., 2006). These data suggest that Moesin acts directly to stabilize Actin microfilament organization in the apical domain rather than acting on the adherens junctions themselves, and that Moesin coordinates vesicle transport to the apical domain during epithelialization (Pilot et al., 2006). A similar relationship between Ve-cadherin and Moesin1 might exist in the ISV during tubulogenesis. The defects observed in Moesin1

knockdown embryos associated with Ve-cadherin junctions could be secondary to the defects in the organization of the Actin cytoskeleton.

Different vessel types utilize different mechanisms for tubulogenesis

Intracellular vacuoles in endothelial cells have been described in vitro and in vivo and are thought to provide apical membrane to the growing lumen during tubulogenesis (Bayless and Davis, 2002; Kamei et al., 2006). In the present study we have used a *Tg(flk1:moesin1-egfp)* transgenic line to follow intracellular vacuoles in vivo during ISV angiogenesis. Our observations provide additional morphological support for a role for vacuoles, and their presence correlates with apical membrane biogenesis during angiogenesis. However, definitive evidence for the involvement of vacuoles in apical membrane biogenesis, and understanding the degree to which they contribute to the apical membrane in vivo, await transgenic lines in which the vacuoles can be definitively followed from their site of origin to the apical membrane. In contrast to our findings, the results from a recent study suggest that during tubulogenesis of the dorsal aorta in mice, vacuoles are not present and that the apical surface is instead defined directly by Ve-cadherin-based junctions and the deposition of Moesin and F-actin between junctional contacts (Strilic et al., 2009). The lack of vacuoles detected in the endothelial cells of the dorsal aorta could reflect the limitations of examining this process in fixed tissue. Using live imaging, we also did not observe large vacuoles during tube formation of the dorsal aorta in the *Tg(flk1:moesin1-egfp)* transgenic line. Consequently, the lack of vacuoles observed during dorsal aorta tubulogenesis could reflect different mechanisms driving tube formation during vasculogenesis and angiogenesis.

Moesin1 is required for ISV tube formation

Consistent with mouse knockout studies (Strilic et al., 2009), our work in zebrafish shows that only minor defects are observed during axial vessel tubulogenesis following knockdown of Moesin1. This is in contrast to near complete failure of the zebrafish ISVs to undergo tubulogenesis. Our observations are similar to analyses of ERM family members in other systems. Knockdown of ERM-1 in *C. elegans*, the only ERM family member present in the genome, results in defects in tubulogenesis of the gut (Gobel et al., 2004; Van Furden et al., 2004). Also, similar to our observations, this effect is possibly mediated through defects in apical junctional remodeling and/or vesicle trafficking. Ezrin is also required in mice for proper villi morphogenesis and secondary lumen formation in the intestine (Saotome et al., 2004). Mouse ezrin has been shown to be required for the fusion of H^+,K^+ ATPase-rich vesicles to the apical membrane in parietal cells of the stomach (Tamura et al., 2005), suggesting that the defects in the intestine could directly relate to disrupted vesicle trafficking. In *Drosophila* photoreceptor cells, Moesin is required for translocation of the transient receptor potential from the rhabdomere membrane to the cytoplasm (Chorna-Ornan et al., 2005), further implicating *Drosophila* Moesin in mediating vesicle trafficking. Based on the localization of Moesin1-EGFP to regions surrounding vacuoles and the apical membrane, we predict that Moesin1 participates in vacuole trafficking to the apical surface.

Moesin1 knockdown embryos displayed defects in the polarization of endothelial cells during ISV tubulogenesis. This defect could be due to disruption in the organization of the Actin cytoskeleton that directs apical/basal cell polarity. In vitro studies in HUVECs indicate that loss of function of Cdc42 and Rac, as well as of their downstream targets Pak2, Pak4, Par3 and the PKC signaling pathway, lead to defects in endothelial tube formation (Koh et al., 2008). These studies suggest that failure to establish apical/basal polarity leads to an inability to initiate tubulogenesis. The endothelial tube formation defects in Moesin1 knockdowns could reflect a primary defect in apical/basal polarity organization of the Actin cytoskeleton, in the formation and stabilization of adherens junctions, or both. Here, we provide the first evidence for a role for the ERM proteins in endothelial tubulogenesis during angiogenesis, and show that Moesin1 and Ve-cadherin function during tubulogenesis in vivo. We suggest that Moesin1 and Ve-cadherin function in endothelial cells in vivo and are required for establishment of apical/basal cell polarity.

Acknowledgements

We thank Drs Kayla Bayless, Kenneth Kramer and Ross Johnson for their careful reading of the manuscript; Dr Darius Balciunas for supplying transposon vectors and the *silent heart* mutant line; Dr Didier Stainier for supplying the *flk1* promoter; Dr Chi-Bin Chien for transposon vectors; Drs Heinz-Georg Belting and Markus Affolter for the Ve-cadherin antibody; Dr Yanhai Yin for the EGFP antibody; and Ms Danhua Zhang for help with molecular cloning. Some strains of zebrafish used in this study were obtained from the Zebrafish International Resource Center, which is supported by grant P40 RR012546 from the NIH-NCRR. This work was supported by NIH/NCI 1R43CA108117-01, the Roy J. Carver Charitable Trust, and Iowa State University start-up funds awarded to J.J.E. Deposited in PMC for release after 12 months.

Competing interests statement

The authors declare no competing financial interests.

Author contributions

Y.W. and J.J.E. designed and carried out the experiments and Y.W., M.M. and J.J.E. wrote the manuscript. M.M. constructed the *Tg(β-actin:rfp)* line. M.S.K. was responsible for statistical analysis of the data. The Moesin1 phenotype was identified and validated in a morpholino-based screen conducted by A.N., J.D.L., S.E.R.-P., K.J.C., S.A.W., S.C.E., P.B.H. and J.J.E.

Supplementary material

Supplementary material for this article is available at
http://dev.biologists.org/lookup/suppl/doi:10.1242/dev.048785/-/DC1

References

Andrew, D. J. and Ewald, A. J. (2010). Morphogenesis of epithelial tubes: insights into tube formation, elongation, and elaboration. *Dev. Biol.* **341**, 34-55.

Bagnat, M., Cheung, I. D., Mostov, K. E. and Stainier, D. Y. (2007). Genetic control of single lumen formation in the zebrafish gut. *Nat. Cell Biol.* **9**, 954-960.

Bayless, K. J. and Davis, G. E. (2002). The Cdc42 and Rac1 GTPases are required for capillary lumen formation in three-dimensional extracellular matrices. *J. Cell Sci.* **115**, 1123-1136.

Bayless, K. J. and Davis, G. E. (2004). Microtubule depolymerization rapidly collapses capillary tube networks in vitro and angiogenic vessels in vivo through the small GTPase Rho. *J. Biol. Chem.* **279**, 11686-11695.

Berryman, M., Franck, Z. and Bretscher, A. (1993). Ezrin is concentrated in the apical microvilli of a wide variety of epithelial cells whereas moesin is found primarily in endothelial cells. *J. Cell Sci.* **105**, 1025-1043.

Blum, Y., Belting, H. G., Ellertsdottir, E., Herwig, L., Luders, F. and Affolter, M. (2008). Complex cell rearrangements during intersegmental vessel sprouting and vessel fusion in the zebrafish embryo. *Dev. Biol.* **316**, 312-322.

Bretscher, A., Edwards, K. and Fehon, R. G. (2002). ERM proteins and merlin: integrators at the cell cortex. *Nat. Rev. Mol. Cell Biol.* **3**, 586-599.

Carmeliet, P., Lampugnani, M. G., Moons, L., Breviario, F., Compernolle, V., Bono, F., Balconi, G., Spagnuolo, R., Oostuyse, B., Dewerchin, M. et al. (1999). Targeted deficiency or cytosolic truncation of the VE-cadherin gene in mice impairs VEGF-mediated endothelial survival and angiogenesis. *Cell* **98**, 147-157.

Chen, J. N., Haffter, P., Odenthal, J., Vogelsang, E., Brand, M., van Eeden, F. J., Furutani-Seiki, M., Granato, M., Hammerschmidt, M., Heisenberg, C. P. et al. (1996). Mutations affecting the cardiovascular system and other internal organs in zebrafish. *Development* **123**, 293-302.

Chorna-Ornan, I., Tzarfaty, V., Ankri-Eliahoo, G., Joel-Almagor, T., Meyer, N. E., Huber, A., Payre, F. and Minke, B. (2005). Light-regulated interaction of

Dmoesin with TRP and TRPL channels is required for maintenance of photoreceptors. *J. Cell Biol.* **171**, 143-152.
Davis, G. E. and Camarillo, C. W. (1996). An alpha 2 beta 1 integrin-dependent pinocytic mechanism involving intracellular vacuole formation and coalescence regulates capillary lumen and tube formation in three-dimensional collagen matrix. *Exp. Cell Res.* **224**, 39-51.
Davis, G. E., Koh, W. and Stratman, A. N. (2007). Mechanisms controlling human endothelial lumen formation and tube assembly in three-dimensional extracellular matrices. *Birth Defects Res. C Embryo Today* **81**, 270-285.
Dejana, E., Orsenigo, F., Molendini, C., Baluk, P. and McDonald, D. M. (2009a). Organization and signaling of endothelial cell-to-cell junctions in various regions of the blood and lymphatic vascular trees. *Cell Tissue Res.* **335**, 17-25.
Dejana, E., Tournier-Lasserve, E. and Weinstein, B. M. (2009b). The control of vascular integrity by endothelial cell junctions: molecular basis and pathological implications. *Dev. Cell* **16**, 209-221.
Ellertsdottir, E., Lenard, A., Blum, Y., Krudewig, A., Herwig, L., Affolter, M. and Belting, H. G. (2009). Vascular morphogenesis in the zebrafish embryo. *Dev. Biol.* **341**, 56-65.
Folkman, J. and Haudenschild, C. (1980). Angiogenesis in vitro. *Nature* **288**, 551-556.
Gobel, V., Barrett, P. L., Hall, D. H. and Fleming, J. T. (2004). Lumen morphogenesis in C. elegans requires the membrane-cytoskeleton linker erm-1. *Dev. Cell* **6**, 865-873.
Gory-Faure, S., Prandini, M. H., Pointu, H., Roullot, V., Pignot-Paintrand, I., Vernet, M. and Huber, P. (1999). Role of vascular endothelial-cadherin in vascular morphogenesis. *Development* **126**, 2093-2102.
Herbert, S. P., Huisken, J., Kim, T. N., Feldman, M. E., Houseman, B. T., Wang, R. A., Shokat, K. M. and Stainier, D. Y. (2009). Arterial-venous segregation by selective cell sprouting: an alternative mode of blood vessel formation. *Science* **326**, 294-298.
Hughes, S. C. and Fehon, R. G. (2007). Understanding ERM proteins-the awesome power of genetics finally brought to bear. *Curr. Opin. Cell Biol.* **19**, 51-56.
Huisken, J. and Stainier, D. Y. (2009). Selective plane illumination microscopy techniques in developmental biology. *Development* **136**, 1963-1975.
Isogai, S., Horiguchi, M. and Weinstein, B. M. (2001). The vascular anatomy of the developing zebrafish: an atlas of embryonic and early larval development. *Dev. Biol.* **230**, 278-301.
Isogai, S., Lawson, N. D., Torrealday, S., Horiguchi, M. and Weinstein, B. M. (2003). Angiogenic network formation in the developing vertebrate trunk. *Development* **130**, 5281-5290.
Jin, S. W., Beis, D., Mitchell, T., Chen, J. N. and Stainier, D. Y. (2005). Cellular and molecular analyses of vascular tube and lumen formation in zebrafish. *Development* **132**, 5199-5209.
Kalen, M., Wallgard, E., Asker, N., Nasevicius, A., Athley, E., Billgren, E., Larson, J. D., Wadman, S. A., Norseng, E., Clark, K. J. et al. (2009). Combination of reverse and chemical genetic screens reveals angiogenesis inhibitors and targets. *Chem. Biol.* **16**, 432-441.
Kamei, M., Saunders, W. B., Bayless, K. J., Dye, L., Davis, G. E. and Weinstein, B. M. (2006). Endothelial tubes assemble from intracellular vacuoles in vivo. *Nature* **442**, 453-456.
Koh, W., Mahan, R. D. and Davis, G. E. (2008). Cdc42- and Rac1-mediated endothelial lumen formation requires Pak2, Pak4 and Par3, and PKC-dependent signaling. *J. Cell Sci.* **121**, 989-1001.
Lawson, N. D. and Weinstein, B. M. (2002). In vivo imaging of embryonic vascular development using transgenic zebrafish. *Dev. Biol.* **248**, 307-318.
Lubarsky, B. and Krasnow, M. A. (2003). Tube morphogenesis: making and shaping biological tubes. *Cell* **112**, 19-28.
Martin-Belmonte, F. and Mostov, K. (2008). Regulation of cell polarity during epithelial morphogenesis. *Curr. Opin. Cell Biol.* **20**, 227-234.
Matsui, T., Maeda, M., Doi, Y., Yonemura, S., Amano, M., Kaibuchi, K. and Tsukita, S. (1998). Rho-kinase phosphorylates COOH-terminal threonines of ezrin/radixin/moesin (ERM) proteins and regulates their head-to-tail association. *J. Cell Biol.* **140**, 647-657.
Montero-Balaguer, M., Swirsding, K., Orsenigo, F., Cotelli, F., Mione, M. and Dejana, E. (2009). Stable vascular connections and remodeling require full expression of VE-cadherin in zebrafish embryos. *PLoS ONE* **4**, e5772.
Nakamura, N., Oshiro, N., Fukata, Y., Amano, M., Fukata, M., Kuroda, S., Matsuura, Y., Leung, T., Lim, L. and Kaibuchi, K. (2000). Phosphorylation of ERM proteins at filopodia induced by Cdc42. *Genes Cells* **5**, 571-581.
Ng, T., Parsons, M., Hughes, W. E., Monypenny, J., Zicha, D., Gautreau, A., Arpin, M., Gschmeissner, S., Verveer, P. J., Bastiaens, P. I. et al. (2001). Ezrin is a downstream effector of trafficking PKC-integrin complexes involved in the control of cell motility. *EMBO J.* **20**, 2723-2741.
Nicoli, S., Ribatti, D., Cotelli, F. and Presta, M. (2007). Mammalian tumor xenografts induce neovascularization in zebrafish embryos. *Cancer Res.* **67**, 2927-2931.
Niggli, V. and Rossy, J. (2008). Ezrin/radixin/moesin: versatile controllers of signaling molecules and of the cortical cytoskeleton. *Int. J. Biochem. Cell Biol.* **40**, 344-349.
Pilot, F., Philippe, J. M., Lemmers, C. and Lecuit, T. (2006). Spatial control of actin organization at adherens junctions by a synaptotagmin-like protein Btsz. *Nature* **442**, 580-584.
Saotome, I., Curto, M. and McClatchey, A. I. (2004). Ezrin is essential for epithelial organization and villus morphogenesis in the developing intestine. *Dev. Cell* **6**, 855-864.
Sehnert, A. J., Huq, A., Weinstein, B. M., Walker, C., Fishman, M. and Stainier, D. Y. (2002). Cardiac troponin T is essential in sarcomere assembly and cardiac contractility. *Nat. Genet.* **31**, 106-110.
Shaw, R. J., Henry, M., Solomon, F. and Jacks, T. (1998). RhoA-dependent phosphorylation and relocalization of ERM proteins into apical membrane/actin protrusions in fibroblasts. *Mol. Biol. Cell* **9**, 403-419.
Siekmann, A. F. and Lawson, N. D. (2007). Notch signalling limits angiogenic cell behaviour in developing zebrafish arteries. *Nature* **445**, 781-784.
Strilic, B., Kucera, T., Eglinger, J., Hughes, M. R., McNagny, K. M., Tsukita, S., Dejana, E., Ferrara, N. and Lammert, E. (2009). The molecular basis of vascular lumen formation in the developing mouse aorta. *Dev. Cell* **17**, 505-515.
Tamura, A., Kikuchi, S., Hata, M., Katsuno, T., Matsui, T., Hayashi, H., Suzuki, Y., Noda, T. and Tsukita, S. (2005). Achlorhydria by ezrin knockdown: defects in the formation/expansion of apical canaliculi in gastric parietal cells. *J. Cell Biol.* **169**, 21-28.
Van Furden, D., Johnson, K., Segbert, C. and Bossinger, O. (2004). The C. elegans ezrin-radixin-moesin protein ERM-1 is necessary for apical junction remodelling and tubulogenesis in the intestine. *Dev. Biol.* **272**, 262-276.
Yang, S., Graham, J., Kahn, J. W., Schwartz, E. A. and Gerritsen, M. E. (1999). Functional roles for PECAM-1 (CD31) and VE-cadherin (CD144) in tube assembly and lumen formation in three-dimensional collagen gels. *Am. J. Pathol.* **155**, 887-895.